Received: Added at production | Revised: Added at production | Accepted: Added at production

DOI: xxx/xxxx

LETTER

The least-square design of minimum-order allpass-based IIR multi-notch filters

Ivan Krstić*

Faculty of Engineering, University of Kragujevac, Kragujevac, Serbia

Correspondence
*Ivan Krstić, 6, Sestre Janjić, Str., 34000 Kragujevac, Serbia. Email: ivan.krstic@kg.ac.rs

Summary

The paper investigates the least-square design of minimum-order infinite impulse response multi-notch filters. Monotonically decreasing nature of the stable allpass filter's phase response, characterizing the allpass-based multi-notch filter, along with the simple relation between coefficients and the phase response of the allpass filter, allows the formulation of the multi-notch filter's magnitude response specifications as the linear equality constraints regarding the positions of notch, left- and right-hand cutoff frequencies. Since the number of such constraints equals triple the number of notch frequencies, while the number of unknown filter coefficients equals double the number of notch frequencies, variable elimination is first performed to ensure that specifications regarding the notch frequencies positions are strictly satisfied. The remaining overdetermined system of linear equations is then solved in the least-square sense, leading to the approximate satisfaction of left- and right-hand cutoff frequencies positions. Proposed design method is also compared with some of the existing infinite impulse response multi-notch filter design methods.

KEYWORDS:
digital multi-notch filter, digital allpass filter, magnitude response, least-square solution

1 | INTRODUCTION

Digital multi-notch filters are required in various applications, among which navigation satellite system receivers [1], preprocessing of the electrocardiogram [2,3] and electromyogram [4] signals, frequency estimation [5,6], and dynamic weighing systems [7]. The purpose of the multi-notch filter is to suppress a certain number of input signal spectral components while passing the other components unchanged. While digital multi-notch filter can be designed as finite-impulse or infinite-impulse response (IIR) filter, the order of the IIR multi-notch filter is considerably lower compared to its finite-impulse response counterpart.

It is well known that very narrow notch-bandwidths of the IIR multi-notch filter can be obtained if poles are placed close to the unit circle. This, however, leads to the prolonged transient response duration [8,9] and lower stability margin [10]. Various IIR multi-notch filter design methods can be found in the literature, while great majority of them can be classified into one of the following three approaches: cascading [11,12], optimal poles placement [13,14,15], and allpass-based [16,17,18,19].

Transfer function of the IIR multi-notch filter, when the cascading approach is considered, is obtained by cascading several IIR single-notch filters. This approach is known to provide good results if notch frequencies are well separated and notch-bandwidths are narrow. Otherwise, uncontrollable gain between notch frequencies occurs [8,17]. Methods of the second approach, ie. the optimal poles placement one, formulates the IIR multi-notch filter design problem as the optimization problem with unknown poles positions. The methods ~~method~~ presented in [14,15] assume ~~assumes~~ known poles radiuses and utilize ~~utilizes~~

particle swarm optimization [14] and the Nelder-Mead simplex method [15] to obtain the unknown phase angles, while in [13] an iterative quadratic programming algorithm is proposed to obtain the unknown poles' locations. The main drawback of the optimal poles placement methods is that maximal passbands gains are not equal.

Regarding the allpass-based approach, specifications of the multiple notch filter's magnitude response are first transformed into the specifications of the corresponding allpass filter's phase response. Then, if the order of the IIR multi-notch filter equals double the number of notch frequencies (which is the minimum value of the IIR multi-notch filter order), a set of linear equations is established and solved for the unknown filter coefficients [16,17,18]. On the other hand, if the order of the IIR multi-notch filter is not minimal, unknown filter coefficients can be determined by solving the quadratic programming optimization problem [19]. The practical success of the minimum-order IIR multi-notch filter allpass-based design methods lies in a fact that these methods are characterized by simple expressions for the coefficients values. Additionally, allpass-based IIR multi-notch filters can be realized using efficient lattice structures.

In this paper, a new design of the minimum-order allpass-based IIR multi-notch filters is proposed. The novelty of this method lies in simultaneous utilization of ~~This method simultaneously utilizes~~ design specifications regarding left- and right-hand cutoff frequencies, while the specifications of the notch frequencies positions are strictly satisfied. Namely, it should be pointed out that existing allpass-based design methods from [17,16], that guarantee the satisfaction of the notch frequencies positions, do not directly utilize either right- or left-hand cutoff frequencies. On the other hand, allpass-based design method from [18] does not directly utilize neither left- nor right-hand cutoff frequencies as it assumes all poles having the same radius. It shows that filters designed using the proposed method can have higher stability margin and lower deviations of the realized left- and right-hand cutoff frequencies from the specified values, compared to minimum-order allpass-based IIR multi-notch filters designed using existing design methods from [16,17].

The rest of the paper is structured as follows. In Sec. 2, an allpass-based IIR multi-notch filter design problem is formulated. A design method is discussed in Sec. 3, while comparison with some of the existing design methods is provided in Sec. 4. Finally, concluding remarks are drawn in Sec. 5.

2 | PROBLEM FORMULATION

Transfer function of the minimum-order allpass-based IIR multi-notch filter is of the following form

$$H(z) = \frac{1}{2}\left[1 + A(z)\right], \tag{1}$$

where $A(z)$ is the stable allpass filter of order $2K$ with single poles

$$A(z) = z^{-2K}\frac{1 + \sum_{k=1}^{2K} p_k z^k}{1 + \sum_{k=1}^{2K} p_k z^{-k}}, \tag{2}$$

and K is the number of notch frequencies. Substituting $z = e^{j\omega}$ in (1), followed by some mathematical manipulations yields

$$H\left(e^{\mathrm{j}\omega}\right) = e^{\mathrm{j}\theta(\omega)/2}\cdot\cos\frac{\theta(\omega)}{2}, \tag{3}$$

where $\theta(\omega)$ is the phase response of the allpass filter $A(z)$:

$$\theta(\omega) = -2K + 2\arctan\frac{\sum_{k=1}^{2K} p_k \sin(k\omega)}{1 + \sum_{k=1}^{2K} p_k\cos(k\omega)}. \tag{4}$$

~~Now, as~~ Specifications of the IIR multi-notch filters comprise K notch frequencies, denoted by $\omega_{n,i}$, $i = 1, 2, \ldots, K$, and K notch-bandwidths $\Delta\omega_i$, for $i = 1, 2, \ldots, K$, specified at attenuation of a dB. Left- and right-hand cutoff frequencies are related to the specified notch-bandwidths as

$$\begin{aligned}\omega_{l,i} &= \omega_{n,i} - \frac{\Delta\omega_i}{2},\\ \omega_{r,i} &= \omega_{n,i} + \frac{\Delta\omega_i}{2},\end{aligned} \tag{5}$$

for $i = 1, 2, \ldots, K$, respectively. ~~, and~~ Therefore, since magnitude response of the IIR multi-notch filter derived from (3) equals

$$\left|H\left(e^{\mathrm{j}\omega}\right)\right| = \left|\cos\frac{\theta(\omega)}{2}\right|, \tag{6}$$

from the monotonically decreasing nature of the stable allpass filter's phase response (while $\theta(0) = 0$ and $\theta(\pi) = -2K\pi$)[11,16], it can be concluded that specifications regarding notch, left- and right-hand cutoff frequencies are satisfied if $\theta(\omega)$ satisfies

$$\theta\left(\omega_{l,i}\right) = -2(i-1)\pi - \varepsilon, \tag{7}$$

$$\theta\left(\omega_{n,i}\right) = -(2i-1)\pi, \tag{8}$$

$$\theta\left(\omega_{r,i}\right) = -2i\pi + \varepsilon, \tag{9}$$

for $i = 1, 2, \ldots, K$, where

$$\varepsilon = 2\arccos 10^{-a/20}. \tag{10}$$

Ideally, the allpass filter's coefficients vector

$$\boldsymbol{p} = \left[p_1\ p_2\ \ldots\ p_{2K}\right]^{\mathrm{T}}, \tag{11}$$

should be determined such that $3K$ equations given by (7), (8) and (9) are satisfied. However, this is not possible, in general, as there are only $2K$ unknown coefficients.

3 | DESIGN METHOD

As the phase response of the allpass filter and its coefficients are related by

$$\sum_{k=1}^{2K} p_k \sin\left(\frac{\theta(\omega)}{2} + (K-k)\omega\right) = -\sin\left(\frac{\theta(\omega)}{2} + K\omega\right), \tag{12}$$

which follows from (4), equations (7), (8) and (9) can be rewritten as

$$\boldsymbol{\Psi}_L \cdot \boldsymbol{p} = \boldsymbol{\gamma}_L, \tag{13}$$

$$\boldsymbol{\Psi}_N \cdot \boldsymbol{p} = \boldsymbol{\gamma}_N, \tag{14}$$

$$\boldsymbol{\Psi}_R \cdot \boldsymbol{p} = \boldsymbol{\gamma}_R, \tag{15}$$

where $\boldsymbol{\Psi}_L = \left[\psi_{ki}^{(L)}\right]$, $\boldsymbol{\Psi}_N = \left[\psi_{ki}^{(N)}\right]$ and $\boldsymbol{\Psi}_R = \left[\psi_{ki}^{(R)}\right]$ are $K \times 2K$ matrices, while $\boldsymbol{\gamma}_L = \left[\gamma_k^{(L)}\right]$, $\boldsymbol{\gamma}_N = \left[\gamma_k^{(N)}\right]$ and $\boldsymbol{\gamma}_R = \left[\gamma_k^{(R)}\right]$ are $K \times 1$ column matrices with elements

$$\begin{aligned} \psi_{ki}^{(L)} &= \sin\left(\omega_{l,k}(K-i) - \frac{\varepsilon}{2}\right), & \gamma_k^{(L)} &= -\sin\left(K\omega_{l,k} - \frac{\varepsilon}{2}\right), \\ \psi_{ki}^{(N)} &= \cos\left(\omega_{n,k}(K-i)\right), & \gamma_k^{(N)} &= -\cos\left(K\omega_{n,k}\right), \\ \psi_{ki}^{(R)} &= \sin\left(\omega_{r,k}(K-i) + \frac{\varepsilon}{2}\right), & \gamma_k^{(R)} &= -\sin\left(K\omega_{r,k} + \frac{\varepsilon}{2}\right). \end{aligned} \tag{16}$$

Obviously, all $3K$ linear equations given in matrix notation by (13), (14) and (15) cannot be simultaneously satisfied since there are only $2K$ unknowns. Hence, following design method is proposed:

a) First, to guarantee exact satisfaction of specifications regarding the notch frequencies positions, (14) is substituted in (13) and (15). In other words, variable elimination is performed. Thus, equations (13) and (15) become

$$\left(\boldsymbol{\Upsilon}_L - \boldsymbol{\Phi}_L \cdot \boldsymbol{\Phi}_N^{-1} \cdot \boldsymbol{\Upsilon}_N\right) \cdot \boldsymbol{p}_x = \boldsymbol{\gamma}_L - \boldsymbol{\Phi}_L \cdot \boldsymbol{\Phi}_N^{-1} \cdot \boldsymbol{\gamma}_N, \tag{17}$$

$$\left(\boldsymbol{\Upsilon}_R - \boldsymbol{\Phi}_R \cdot \boldsymbol{\Phi}_N^{-1} \cdot \boldsymbol{\Upsilon}_N\right) \cdot \boldsymbol{p}_x = \boldsymbol{\gamma}_R - \boldsymbol{\Phi}_R \cdot \boldsymbol{\Phi}_N^{-1} \cdot \boldsymbol{\gamma}_N, \tag{18}$$

where $\boldsymbol{\Upsilon}_L$, $\boldsymbol{\Upsilon}_N$, $\boldsymbol{\Upsilon}_R$, $\boldsymbol{\Phi}_L$, $\boldsymbol{\Phi}_N$ and $\boldsymbol{\Phi}_R$ are $K \times K$ matrices related to $\boldsymbol{\Psi}_L$, $\boldsymbol{\Psi}_N$ and $\boldsymbol{\Psi}_R$ as

$$\boldsymbol{\Psi}_L = \left[\boldsymbol{\Phi}_L\ \boldsymbol{\Upsilon}_L\right], \quad \boldsymbol{\Psi}_N = \left[\boldsymbol{\Phi}_N\ \boldsymbol{\Upsilon}_N\right], \quad \boldsymbol{\Psi}_R = \left[\boldsymbol{\Phi}_R\ \boldsymbol{\Upsilon}_R\right], \tag{19}$$

while $\boldsymbol{p}$ is partitioned as

$$\boldsymbol{p} = \begin{bmatrix} \boldsymbol{p}_e \\ \boldsymbol{p}_x \end{bmatrix}, \tag{20}$$

and $\boldsymbol{p}_e$ is the $K \times 1$ vector of eliminated coefficients

$$\boldsymbol{p}_e = \boldsymbol{\Phi}_N^{-1} \cdot \left(\boldsymbol{\gamma}_N - \boldsymbol{\Upsilon}_N \cdot \boldsymbol{p}_x\right), \tag{21}$$

note (14).

b) Second, system of $2K$ equations in K unknowns, given by (17) and (18), is solved in the least-square sense:

$$\boldsymbol{p}_x = \begin{bmatrix} \boldsymbol{\Upsilon}_L - \boldsymbol{\Phi}_L \cdot \boldsymbol{\Phi}_N^{-1} \cdot \boldsymbol{\Upsilon}_N \\ \boldsymbol{\Upsilon}_R - \boldsymbol{\Phi}_R \cdot \boldsymbol{\Phi}_N^{-1} \cdot \boldsymbol{\Upsilon}_N \end{bmatrix}^{\dagger} \cdot \begin{bmatrix} \boldsymbol{\gamma}_L - \boldsymbol{\Phi}_L \cdot \boldsymbol{\Phi}_N^{-1} \cdot \boldsymbol{\gamma}_N \\ \boldsymbol{\gamma}_L - \boldsymbol{\Phi}_L \cdot \boldsymbol{\Phi}_N^{-1} \cdot \boldsymbol{\gamma}_N \end{bmatrix}, \tag{22}$$

where † denotes Moore–Penrose inverse. Therefore, specifications of the left- and right-hand cutoff frequencies are approximately satisfied.

An interesting case occurs when specifications of the IIR multi-notch filter are such that $\omega_{n,k} = \pi - \omega_{n,K-k+1}$ and $\Delta\omega_k = \Delta\omega_{K-k+1}$ for $k = 1, 2, \ldots, K$, ie. when there is a symmetry of the design specifications about $\omega = \pi/2$. In this case it shows that utilization of the proposed IIR multi-notch filter design method yields $p_1 = p_2 = \cdots = p_{2K-1} = 0$, that is, only K multiplications are required by the IIR multi-notch filter.

4 | COMPARISON WITH THE EXISTING DESIGN METHODS

Proposed design method is compared to existing minimum-order allpass-based IIR multi-notch filter design methods from [16,17] that guarantee the satisfaction of notch frequencies positions. While these methods consider 3 dB notch-bandwidths, they can be generalized to a case of an arbitrary attenuation value at which notch-bandwidths are specified. Note that such generalization is not possible for the design method presented in [18], as the radius of the poles is derived from the 3 dB notch-bandwidths and it is assumed that identical notch-bandwidths result in all poles having the same radius. A brief description of methods from [16,17], used for comparison with the proposed one follows:

1) Utilization of the *Method I* from [17] guarantees exact satisfaction of specifications regarding the positions of notch and left-hand cutoff frequencies. This method is the same as method presented in [16], however limitations regarding the tangent operations are overcame. Actually, after some mathematical manipulations performed to equations characterizing *Method I* in [17], one can obtain equations (13) and (14). Therefore, vector $\boldsymbol{p}$, that correspond to the transfer function obtained by utilizing the generalization of *Method I* [17] to an arbitrary attenuation value at which notch-bandwidths are specified, is determined by

$$\boldsymbol{p} = \begin{bmatrix} \boldsymbol{\Psi}_L \\ \boldsymbol{\Psi}_N \end{bmatrix}^{-1} \cdot \begin{bmatrix} \boldsymbol{\gamma}_L \\ \boldsymbol{\gamma}_N \end{bmatrix}. \tag{23}$$

2) Utilization of the *Method II* from [17] guarantees exact satisfaction of specifications regarding the positions of notch and right-hand cutoff frequencies. Similar to the previous case, it shows that vector $\boldsymbol{p}$, that correspond to the transfer function obtained by utilizing the generalization of *Method II* [17] to an arbitrary attenuation value at which notch-bandwidths are specified, can be determined as a solution to the system of equations given by (14) and (15), ie.

$$\boldsymbol{p} = \begin{bmatrix} \boldsymbol{\Psi}_N \\ \boldsymbol{\Psi}_R \end{bmatrix}^{-1} \cdot \begin{bmatrix} \boldsymbol{\gamma}_N \\ \boldsymbol{\gamma}_R \end{bmatrix}. \tag{24}$$

While *Method I* from [17] does not directly utilize the right-hand cutoff frequencies, ie. (15), *Method II* from [17] does not directly utilize left-hand cutoff frequencies, ie. (13). In this sense, one can treat the proposed design method as the 'missing' one in [17], since both (13) and (15) are simultaneously utilized in the design process.

Filter designed using proposed and existing allpass-based design methods from [16,17] are compared in terms of the maximum pole radius $\rho_{\max}$, ~~and~~ relative deviations of the realized left- and right-hand cutoff frequencies, denoted by $\omega'_{l,i}$ and $\omega'_{r,i}$, from the specified values: $\delta\omega_{l,i} = \left(\omega'_{l,i}/\omega_{l,i} - 1\right) \cdot 100\%$ and $\delta\omega_{r,i} = \left(\omega'_{r,i}/\omega_{r,i} - 1\right) \cdot 100\%$, respectively, and realized notch-bandwidths $\Delta\omega'_i = \omega'_{r,i} - \omega'_{l,i}$. Note that if $\delta\omega_{l,i} \geq 0$ or $\delta\omega_{r,i} \leq 0$ specifications are exactly or over satisfied at i-th left- or right-hand cutoff frequency, respectively, otherwise specifications are under satisfied. On the other hand, lower maximum pole radius leads to the shorter transient response duration [8,9] and higher stability margin [10]. Obviously, $\delta\omega_{l,i} = 0$ for $i = 1, 2, \ldots, K$, if filters are designed using *Method I* [17], while $\delta\omega_{r,i} = 0$ for $i = 1, 2, \ldots, K$, if *Method II* [17] utilized.

As the first example, following specifications of the IIR multi-notch filter are considered: $\omega_{n,1} = 0.3\pi$, $\omega_{n,2} = 0.7\pi$, $\Delta\omega_1 = \Delta\omega_2 = 0.1\pi$, $a = 2$ dB. Relative deviations of realized left- and right-hand cutoff frequencies from specified ones in percents, $\delta\omega_{l,i}$ and $\delta\omega_{r,i}$, and realized notch-bandwidths $\Delta\omega'_i$, for $i = 1, 2$, as well as the maximum pole radius of IIR multi-notch filters designed using proposed and existing design methods from [17] are given in Tab. 1. As can be observed, specifications regarding first left- and second right-hand cutoff frequencies are under satisfied by 0.9% and 0.3%, respectively, when proposed design method utilized, while specifications regarding second right- and first left-hand cutoff frequencies are under satisfied by 0.58% and 1.75%, respectively, when *Methods I* and *II* [17] considered. Therefore, as for the first example, IIR multi-notch filter designed using *Method I* [17] outperforms the other two filters. On the other, a filter designed using the proposed design method has the highest stability margin, ie. the lowest maximum pole radius, and outperforms the filter designed using *Method II* [17]. Furthermore, realized notch-bandwidths of the filter designed using the proposed design method are narrower than the specified values, which is not the case when design methods from [17] are considered.

TABLE 1 Example 1. Relative deviations of realized left- and right-hand cutoff frequencies from the specified ones in percents, realized notch-bandwidths, and maximum pole radii of IIR multi-notch filters designed using proposed and existing design methods from [17].

	Proposed, $\rho_{\max} = 0.8814$			*Method I* [17], $\rho_{\max} = 0.8875$			*Method II* [17], $\rho_{\max} = 0.8875$		
i	$\delta\omega_{l,i}$	$\delta\omega_{r,i}$	$\Delta\omega_i'/\pi$	$\delta\omega_{l,i}$	$\delta\omega_{r,i}$	$\Delta\omega_i'/\pi$	$\delta\omega_{l,i}$	$\delta\omega_{r,i}$	$\Delta\omega_i'/\pi$
1	−0.90	−0.78	0.0995	0	−1.58	0.0945	−1.75	0	0.1044
2	0.42	0.30	0.0995	0	0.58	0.1044	0.85	0	0.0945

As the second example, following specifications of the IIR multi-notch filter are considered: $\omega_{n,1} = 0.2\pi$, $\omega_{n,2} = 0.4\pi$, $\omega_{n,3} = 0.7\pi$, $\Delta\omega_1 = \Delta\omega_2 = \Delta\omega_3 = 0.1\pi$, $a = 2.2$ dB. $\delta\omega_{l,i}$, ~~and~~ $\delta\omega_{r,i}$ and $\Delta\omega_i'$ for $i = 1, 2, 3$, and $\rho_{\max}$ that correspond to the IIR multi-notch filters designed using proposed and existing design methods from [17] are given in Tab. 2. For this specifications set, filter designed using the proposed design method outperforms both filters designed using existing methods from [17], as relative deviations of cutoff frequencies where specifications are under satisfied are less than 0.85% compared to 2.58% and 6.09% when *Methods I* and *II* [17] utilized, respectively. Furthermore, filter obtained using the proposed design method also has the highest stability margin and its realized notch-bandwidths are narrower than the specified ones, which is not the case when design methods from [17] are considered.

TABLE 2 Example 2. Relative deviations of realized left- and right-hand cutoff frequencies from the specified ones in percents, realized notch-bandwidths, and maximum pole radii of IIR multi-notch filters designed using proposed and existing design methods from [17].

	Proposed, $\rho_{\max} = 0.8811$			*Method I* [17], $\rho_{\max} = 0.8855$			*Method II* [17], $\rho_{\max} = 0.8929$		
i	$\delta\omega_{l,i}$	$\delta\omega_{r,i}$	$\Delta\omega_i'/\pi$	$\delta\omega_{l,i}$	$\delta\omega_{r,i}$	$\Delta\omega_i'/\pi$	$\delta\omega_{l,i}$	$\delta\omega_{r,i}$	$\Delta\omega_i'/\pi$
1	−0.13	−4.28	0.0895	0	−6.22	0.0845	−6.09	0	0.1091
2	3.54	−0.37	0.0859	0	1.92	0.1086	4.85	0	0.0830
3	1.25	0.85	0.0982	0	2.59	0.1195	2.23	0	0.0855

As the third example, following specifications of the IIR multi-notch filter are considered: $\omega_{n,1} = 0.1$, $\omega_{n,2} = 0.2\pi$, $\omega_{n,3} = 0.4\pi$, $\omega_{n,4} = 0.8\pi$, $\Delta\omega_1 = \Delta\omega_2 = 0.06\pi$, $\Delta\omega_3 = 0.08\pi$, $\Delta\omega_4 = 0.1\pi$, $a = 3$ dB. $\delta\omega_{l,i}$, ~~and~~ $\delta\omega_{r,i}$ and $\Delta\omega_i'$ for $i = 1, 2, 3, 4$, and $\rho_{\max}$ that correspond to the IIR multi-notch filters designed using proposed and existing design methods from [17] are given in Tab. 3. For the considered IIR multi-notch filter specifications, proposed design method outperforms by far the other two considered methods since specifications are under satisfied only by 0.02% and only at the fourth left-hand cutoff frequency. Furthermore, realized notch-bandwidths of the filter designed using the proposed design method are narrower or equal to the specified notch-bandwidths, which is not the case when design methods from [17] are utilized. On the other hand, specifications are under satisfied by the other two filters at three cutoff frequencies, note Tab. 3. In this example, however, filter obtained using the proposed design method has the lowest stability margin. Magnitude responses of obtained filters in dB are shown in Fig. 1.

TABLE 3 Example 3. Relative deviations of realized left- and right-hand cutoff frequencies from the specified ones in percents, realized notch-bandwidths, and maximum pole radii of IIR multi-notch filters designed using proposed and existing design methods from [17].

	Proposed, $\rho_{\max} = 0.9396$			*Method I* [17], $\rho_{\max} = 0.9088$			*Method II* [17], $\rho_{\max} = 0.9287$		
i	$\delta\omega_{l,i}$	$\delta\omega_{r,i}$	$\Delta\omega_i'/\pi$	$\delta\omega_{l,i}$	$\delta\omega_{r,i}$	$\Delta\omega_i'/\pi$	$\delta\omega_{l,i}$	$\delta\omega_{r,i}$	$\Delta\omega_i'/\pi$
1	13.92	−11.11	0.0358	0	−8.15	0.0494	−6.32	0	0.0644
2	6.94	−3.86	0.0393	0	4.55	0.0705	7.85	0	0.0467
3	1.34	−0.42	0.0770	0	4.93	0.1017	3.32	0	0.0680
4	−0.02	−0.02	0.1000	0	0.48	0.1041	0.13	0	0.0990

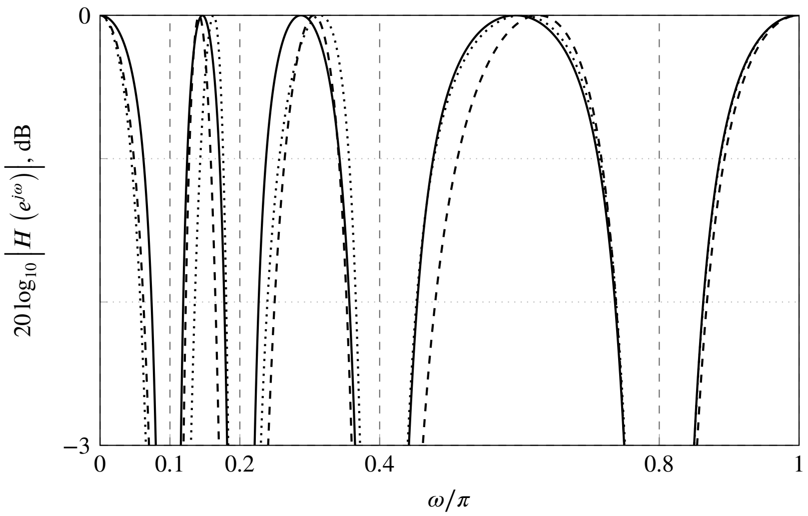

FIGURE 1 Example 3. Magnitude responses of filters designed using proposed (solid), *Method I* [17] (dashed) and *Method II* [17] (dotted line).

5 | CONCLUSION

The least-square design of minimum-order allpass-based IIR multi-notch filter is presented in the paper. Specifications of the multi-notch filter's magnitude response are first formulated as linear equality constraints, and variable elimination is performed to guarantee exact satisfaction of the notch frequencies positions. The remaining overdetermined system of linear equations is then solved in the least-square sense. As opposed to the existing allpass-based design methods from [16,17], specifications regarding the left- and right-hand cutoff frequencies are simultaneously utilized by the proposed design method. Results of comparison with the existing minimum-order allpass-based IIR multi-notch filter design methods suggest that utilization of the proposed method can result in transfer functions having higher stability margins (ie. ~~lower pole radiuses~~ lower maximum radius of the poles), ~~and~~ lower relative deviations of realized left- and right-hand cutoff frequencies from the specified ones, and narrower realized notch-bandwidths than the specified ones.

Financial disclosure

None reported.

Conflict of interest

The author declare no potential conflict of interests.

References

1. Zhao H, Hu Y, Sun H, Feng W. A BDS interference suppression technique based on linear phase adaptive IIR notch filters. *Sensors* 2018; 18(5): 1515.

2. Mahendran RK, Velusamy P, Pandian P. An efficient priority-based convolutional auto-encoder approach for electrocardiogram signal compression in Internet of Things based healthcare system. *Transactions on Emerging Telecommunications Technologies* 2021; 32(1): e4115.

3. Appathurai A, Carol JJ, Raja C, et al. A study on ECG signal characterization and practical implementation of some ECG characterization techniques. *Measurement* 2019; 147: 106384.

4. Piskorowski J. Time-efficient removal of power-line noise from EMG signals using IIR notch filters with non-zero initial conditions. *Biocybernetics and Biomedical Engineering* 2013; 33(3): 171–178.

5. Elasmi-Ksibi R, Cherif S, López-Valcarce R, Besbes H. Closed-form real single-tone frequency estimator based on a normalized IIR notch filter. *Signal Processing* 2010; 90(6): 1905–1915.

6. Savaresi SM, Bittanti S, So H. Closed-form unbiased frequency estimation of a noisy sinusoid using notch filters. *IEEE Transactions on automatic control* 2003; 48(7): 1285–1292.

7. Sun B, Teng Z, Hu Q, Lin H, Tang S. Periodic noise rejection of checkweigher based on digital multiple notch filter. *IEEE Sensors Journal* 2020; 20(13): 7226–7234.

8. Tan L, Jiang J, Wang L. Pole-radius-varying IIR notch filter with transient suppression. *IEEE transactions on instrumentation and measurement* 2012; 61(6): 1684–1691.

9. Wang XL, Ge YJ, Zhang JJ, Song QJ. Discussion on the -3 dB rejection bandwidth of IIR notch filters. In: . 1. IEEE. ; 2002: 151–154.

10. Lang MC. Weighted least squares IIR filter design with arbitrary magnitude and phase responses and specified stability margin. In: IEEE. ; 1998: 82–86.

11. Regalia PA, Mitra SK, Vaidyanathan P. The digital all-pass filter: A versatile signal processing building block. *Proceedings of the IEEE* 1988; 76(1): 19–37.

12. Pei SC, Lu WY, Guo BY. Pole–zero assignment of all-pass-based notch filters. *IEEE Transactions on Circuits and Systems II: Express Briefs* 2016; 64(4): 477–481.

13. Tseng CC, Pei SC. Stable IIR notch filter design with optimal pole placement. *IEEE Transactions on Signal processing* 2001; 49(11): 2673–2681.

14. Wang Q, Kundur D, Yuan H, Liu Y, Lu J, Ma Z. Noise suppression of corona current measurement from HVdc transmission lines. *IEEE transactions on instrumentation and measurement* 2015; 65(2): 264–275.

15. Wang Q, Gu X, Liu Y, Yuan H. Digital Multiple Notch Filter Design with Nelder-Mead Simplex Method. *IEICE TRANSACTIONS on Fundamentals of Electronics, Communications and Computer Sciences* 2017; 100(1): 259–265.

16. Pei SC, Tseng CC. IIR multiple notch filter design based on allpass filter. *IEEE Transactions on Circuits and Systems II: Analog and Digital Signal Processing* 1997; 44(2): 133–136.

17. Wang Q, Kundur D. A generalized design framework for IIR digital multiple notch filters. *EURASIP Journal on Advances in Signal Processing* 2015; 2015(1): 1–13.

18. Wang Q, Gu X, Lin J. Adaptive notch filter design under multiple identical bandwidths. *AEU-International Journal of Electronics and Communications* 2017; 82: 202–210.

19. Nikolić S, Krstić I, Stančić G. Noniterative design of IIR multiple-notch filters with improved passband magnitude response. *International Journal of Circuit Theory and Applications* 2018; 46(12): 2561–2567.

□